

# Influence of the nonlinear bias dependence of the barrier height on measured Schottky-barrier contact parameters

V. G. Bozhkov and A. V. Shmargunov<sup>a)</sup>*Joint-Stock Company Research Institute of Semiconductor Devices, 634034, Tomsk, Russia*

(Received 9 March 2011; accepted 4 April 2011; published online 10 June 2011)

A numerical investigation of current-voltage characteristics (IVCs) of the ideal metal-semiconductor Schottky-barrier contact (SBC) metal-n-GaAs in the wide range of temperatures, contact diameters and doping levels considering the influence of image force and tunneling effects is presented. The analysis is carried out on the basis of model, taking into account the nonlinear bias dependence of the barrier height (generally, effective one) and assuming that the SBC parameters are determined at constant (specified) current value in the temperature or contact diameter ranges, which corresponds practically to experimental conditions of measurement of SBC parameters. It is shown that such SBCs have behavior peculiarities typical for most real contacts: the “low temperature anomaly” (the ideality factor  $n$  increase and the barrier height  $\phi_{bm}$  (measured by the saturation current) decrease with temperature decrease), edge effects (increase of  $n$  and decrease of  $\phi_{bm}$  with contact diameter decrease), the inverse connection between  $\phi_{bm}$  and  $n$ , when the growth of one of them is followed by the decrease of the other. A simple and very precise analytic representation of the IVC is given for the SBC in wide temperature and doping level ranges. This representation agrees closely with known experimental results. The high-accuracy method of the barrier height determining is proposed on this basis. © 2011 American Institute of Physics. [doi:10.1063/1.3587233]

## I. INTRODUCTION

It is well known that despite of the well defined mechanism of the current transport in rather perfect Schottky barrier contacts (which is the thermoionic emission over the barrier<sup>1</sup>), their current-voltage ( $I$ - $V$ ) characteristics (IVCs) in many cases have significant deviations from the ideal (theoretical) behavior. These are the remarkable difference between the barrier heights defined by  $I$ - $V$ - and  $C$ - $V$ -methods ( $\phi_b$  and  $\phi_{bc}$ , respectively),<sup>1</sup> presence of the edge effects (dependence of the contact characteristics on contact dimensions),<sup>2-4</sup> inverse connection between the barrier height and ideality factor  $n$  for single-type contacts fabricated under the same conditions<sup>5,6</sup> and, finally, well known “low temperature anomaly” of IVC: increase in ideality factor and decrease in barrier height  $\phi_{bm}$  with temperature decrease, so that their product  $\phi_{bn} \equiv n\phi_{bm}$  is a weak function of temperature and close to the real barrier height defined by other methods.<sup>7-12</sup> Here  $\phi_{bm}$  is the barrier height measured by the saturation current. We exclude from consideration anomalies of reverse IVCs, which are far more complex to explain (excluding separate cases of more perfect contacts) because of their high sensitivity to manufacture technologies. All specified deviations are known for some decades; however, their nature is still a subject for discussion up to date. Of special interest is the “low temperature anomaly” of IVC, since underlying reasons can be the key to the explanation of other deviations in the IVC behavior.

A number of attempts to explain the nature of the “low temperature anomaly” in SBCs are known. These include

hypotheses about increasing the role of recombination current (in the SB area) with temperature decreasing,<sup>1,3-15</sup> the influence of deep traps in the subsurface layer of semiconductor,<sup>5</sup> local areas with high density of impurities, structure defects, elements of surface relief, etc. (some of them can act as centers of local thermoionic-field emission<sup>16,17</sup>), inhomogeneous distribution of interface states (IS) in the contact,<sup>18</sup> energy dependence of the IS density communicating with semiconductor,<sup>19,20</sup> and, finally, about the influence of laterally inhomogeneous distribution of the barrier height. In the latter case, inhomogeneities of at least three types were considered. The first one is the inhomogeneity in the form of local (primarily peripheral) lowering of the barrier height under the effect of elastic mechanical stresses in the contact and possibly other factors.<sup>19,21,22</sup> The second one is in the form of Gaussian distribution (valid for continuous and smooth barrier height changing), parameters of which (standard deviation and average barrier height) are the bias dependent functions,<sup>10</sup> and the third type of the inhomogeneity is in the form of so-called “saddle points,”<sup>23,24</sup> which appear in the contact under specific conditions, when small patches with the low barrier height are surrounded by the area with large barrier height.

Over the last two decades, the idea on the lateral barrier height inhomogeneity becomes the most popular in explanation of the low temperature and other SBC anomalies, though it is difficult to speak about its direct confirmation. We believe that a balanced approach to this problem is required, which should take into account the role of other reasons stimulating the SBC anomalies. In our opinion, the most common approach can be realized on the basis of taking into consideration the nonlinear

<sup>a)</sup>Electronic mail: tohsh@list.ru.

bias dependence of the barrier height (in general not only real but also effective one) manifesting itself in the bias dependence of the IVC ideality factor:  $n = n(V)$ .<sup>20,25,26</sup> The adequacy of this approach is based on the real barrier height nonlinearity which is characteristic in a varying degree to all SBCs without exception. Essentially, this is a fundamental property of SBCs. However, for high quality contacts the manifestation of the nonlinear  $\phi_b(V)$  dependence or  $n(V)$ -dependence seems to be weak in  $I$ - $V$  characteristics. This is due to the fact that at relatively high temperatures, the manifestation is weak because of small (close to 1) values of  $n$ , and at low temperatures, we deal with IVC in a relatively narrow bias voltage range (because of a problem of measuring ultra low currents), where it can also be weak.

As it was shown, a number of possible reasons stimulating the SBC anomalies can be considered within the limits of common approach. These are, for example, inhomogeneous (by energy) distribution of interface states communicating with semiconductor in the contact with an intermediate insulating layer and IS,<sup>19,20,27</sup> subsurface (near the interface) states distributed over the coordinate and energy in the intimate contact,<sup>28</sup> barrier height inhomogeneities,<sup>17,29</sup> image force in the ideal contact, the influence of which is an immediate cause of the barrier height nonlinearity,<sup>30</sup> and even the tunnel effect,<sup>31</sup> the low temperature behavior of which seems to have natural physical explanation. Other possible reasons of barrier height nonlinearity are mentioned, for example, in the work.<sup>32</sup>

There is necessary condition for the implementation of the considered approach. It consists in the requirement that the measurement of SBC parameters ( $n$  and  $\phi_{bm}$ ) in the temperature and contact diameter range should be carried out at the constant (specified) current value.<sup>20,25,26</sup> Essentially, this requirement is usually fulfilled automatically (first of all, under measurements in the temperature range). However, up to now, it was not taken into account in calculations and experimental investigations (except some works by one of the authors).

In this work, on the example of the ideal SBC considering only the image force and tunneling effects (the fundamental effects), we show that on the basis of the concept of the nonlinear bias dependence of the barrier height (in this case, an effective barrier height), it is possible to explain and describe not only the “low temperature anomaly” of the IVC, but also the edge effects in the contact (the dependence of the ideality factor and the measured barrier height on the contact diameter) and inverse connection between  $n$  and  $\phi_{bm}$ . Before, this connection was explained only by the barrier height inhomogeneity in the form of “saddle points.”<sup>6,23,24</sup> In the considered ideal SBCs, it is explained by the fluctuations of the impurity concentration in the semiconductor. It seems to be evident, that in real contacts there is a far more wide set of factors whose fluctuations can stimulate the inverse connection between  $n$  and  $\phi_{bm}$ .

It is shown also, that the IVC of the considered contacts can be described in a wide range of impurity concentrations and temperatures with a simple analytical expression, which includes only measured contact parameters that have a direct

physical meaning. This makes it possible to propose the high-accuracy method for the barrier height determining.

## II. BASIC RELATIONS

Let us consider the idealized contact without intermediate layer and surface (interface) electronic states. The deviation of the IVC of this contact from the ideal one corresponding to the thermoionic emission mechanism is due to the influence of image force, which cause the nonlinear increase of the barrier height with the bias voltage increase, and to the tunneling through the barrier.<sup>1</sup> Considering these factors, the IVC can be presented in the following well-known form:<sup>33,34</sup>

$$I = \frac{AR^*T}{k} \exp\left(-\frac{q\phi_s}{kT}\right) \int_0^\infty T_t(E) \exp\left(-\frac{E}{kT}\right) dE \times \left[1 - \exp\left(-\frac{qV - IR_s}{kT}\right)\right], \quad (1)$$

where  $A$  is the contact area,  $R^*$  is the effective Richardson constant,  $T$  is the absolute temperature,  $k$  is the Boltzmann constant,  $q$  is the electron charge,  $R_s$  is the contact series resistance,  $q\phi_s = E_C - E_{Fs} = kT \ln(N_C/N_D)$  is the energy interval between the conduction band bottom ( $E_C$ ) and the Fermi level ( $E_{Fs}$ ) in the volume of the  $n$ -type semiconductor;  $N_C$  is the effective state density in the conduction band,  $N_D$  is a concentration of donor impurity in the semiconductor, and  $T_t(E)$  is a barrier transmission coefficient in the WKB-approximation:

$$T_t(E) = \exp\left(-\frac{4\pi}{h} \int_{x_1}^W \{2m^*[qV(x) - E]\}^{1/2} dx\right). \quad (2)$$

Here  $h$  is the Plank constant,  $m^*$  is the effective electron mass,  $V(x)$  is the potential profile in the barrier calculated from the solution of the Poisson equation,  $x_1$  is the barrier width for the tunneling electron defined by its energy. Allowing for the image force effect, the potential profile is presented as follows:<sup>1</sup>

$$qV(x) = \frac{qN_D}{2\epsilon_s} x^2 - \frac{q^2}{16\pi\epsilon_s(W-x)}, \quad (3)$$

where  $\epsilon_s = \epsilon_{s0}\epsilon_0$  is the semiconductor dielectric permittivity (for simplicity, it is assumed that the high frequency permittivity is equal to the static one<sup>1</sup>),  $\epsilon_0$  is the vacuum dielectric permittivity,  $W$  is the barrier width. (The barrier boundary with the quasineutral volume is selected as the reference point  $x=0$ .) For electron energies meeting the condition  $E \geq q(V_m - V)$ , the transmission coefficient was taken equal to 1.  $V_m$  is the maximum value of the potential in the barrier.

At the same time, the forward IVC of the considered contact can be presented in the most common form:

$$I = AR^*T^2 \exp\left[-\frac{q\phi_{bef}(V)}{kT}\right] \exp\left(\frac{qV - IR_s}{kT}\right), \quad (4)$$

where  $\phi_{bef}(V)$  is the effective barrier height. For this representation of IVC, it was usually supposed that the barrier

height is a weak linear function of bias.<sup>1</sup> However, we take into consideration its nonlinearity, that is why the ideality factor of IVC, which is defined as:<sup>1</sup>

$$n(V) = \frac{q}{kT} \frac{dV}{d \ln I} = \left[ 1 - \frac{d\varphi_{bef}(V)}{dV} \right]^{-1} \quad (5)$$

or

$$n(I) = 1 + \frac{q}{kT} \frac{d\varphi_{bef}(I)}{d \ln I}, \quad (5A)$$

becomes the bias (current) function. The known IVC approximation, with which the ideality factor and the barrier height values are defined, is given by the expression:

$$\begin{aligned} I &= AR^*T^2 \exp \left[ -\frac{q\varphi_{bm}(V)}{kT} \right] \exp \left[ \frac{qV}{n(V)kT} \right] \\ &= I_s \exp \left[ \frac{qV}{n(V)kT} \right]. \end{aligned} \quad (6)$$

Here  $\varphi_{bm}(V)$  is the barrier height measured from (6) by saturation current. Parameters  $n$  and  $\varphi_{bm}$  specify the IVC (4) at a bias voltage  $V$ , at which the IVC (6) is the tangent to the IVC (4) in the semilogarithmic scale.<sup>25,26</sup> Comparison of the IVCs (4) and (6) (equating at the tangency point) allows to relate the effective barrier height  $\varphi_{bef}(V)$  with the measured one  $\varphi_{bm}(V)$ .

But before making this comparison, it is necessary to take into consideration an important circumstance concerning the choice of the tangency point. As it was mentioned above, we suppose that the contact parameters (the ideality factor and barrier height) are measured at a certain current value in the whole range of examined temperatures. Usually, the fulfillment of this condition (the condition of the current constancy) is very important (first, it was emphasized in Refs. 19 and 20), since it reflects the real (experimental) situation: at all temperatures, the IVC measurements are usually performed in the same or close current ranges. It is precisely this condition, which gives the possibility to receive simple and convenient relationships for the determination of the SBC parameters. Note also, that, how it will be shown, the deviation from the above condition in the limits ( $10^{-4} - 10^{-6}$ ) A does not cause essential changes in the results of our calculations.

Returning to the abovementioned, the relationship between the effective and measured barrier heights at the specified current  $I$  can be presented as:<sup>25,26</sup>

$$\varphi_{bl} = n\varphi_{bm} - (n-1) \frac{kT}{q} \ln \frac{AR^*T^2}{I}, \quad (7)$$

where  $\varphi_{bl} \equiv \varphi_{bef}$ . It is natural that the ideality factor corresponds also to the specified current  $I$ , which is really (under measurements) chosen usually in the range of  $10^{-6} - 10^{-4}$  A. The meaning of the relationship (7) is obvious: only for an ideal contact ( $n = 1$ ), the measured barrier height is equal to the true one. With the deviation from ideality (with the increase of  $n$ ), the difference between them increases and the

barrier height  $\varphi_{bl}$  becomes the effective one. Note, that at  $n = \text{const}$ ,  $\varphi_{bm}$  is independent of the current (bias) and becomes equal to zero-bias barrier height  $\varphi_b(V = 0) \equiv \varphi_{b0}$ . In flat-band conditions (at  $n = \text{const}$ ), the expression (7) for  $\varphi_{bl}$  transforms into the known expression for the flat-band barrier height  $\varphi_{bf}$  obtained for the ordinary real contacts:<sup>25,26,35</sup>

$$\varphi_{bf} = n\varphi_{b0} - (n-1)\varphi_s. \quad (8)$$

In the absence of tunnel effect (such situations were considered for the estimation of the relative role of image force and tunneling effects), the IVC was calculated from Eq. (4), where the true barrier height  $\varphi_{bi}$  considering only image force effect was used instead of the effective one. It was defined from the maximum value of the potential  $V_m$  calculated according to (3) with allowance for the  $\varphi_s$ :  $\varphi_{bi} = V_m + \varphi_s$ .

### III. CALCULATION RESULTS AND DISCUSSION

The calculation procedure of the measured contact parameters at specified SBC construction parameters (the material characteristics, contact area, doping level, barrier height without considering the influence of image force effect) includes:

- (1) calculation of  $I$ - $V$ -characteristics according to Eqs. (1)–(3);
- (2) determination of the ideality factor by Eq. (5) using the numerical differentiation of the IVC (1) at the specified current  $I$  and the saturation current, from Eq. (6) as:

$$I_s = I \exp \left( -\frac{qV}{nkT} \right); \quad (9)$$

- (3) determination of the barrier height  $\varphi_{bm}$  (named as the barrier height measured using the saturation current) from Eq. (6) as:

$$\varphi_{bm} = \frac{kT}{q} \ln \left( \frac{AR^*T^2}{I_s} \right) \quad (10)$$

with the specified value of the Richardson constant;

- (4) determination of the effective barrier height  $\varphi_{bl}$  from Eq. (7) with the use of the calculated values  $n$  and  $\varphi_{bm}$  at a specified current.

This procedure was performed to get a comprehensive idea on the behavior of SBC parameters in wide temperature, contact diameter and doping density ranges, which allowed to make new and more common conclusions on SBC properties.

It is easy to make sure that Eq. (7) connecting the effective (or true) barrier height with the measured one is the key equation for the analysis of reasons for the abnormal low temperature dependences  $n(T)$  and  $\varphi_{bm}(T)$  and edge effects [dependences  $n(d)$  and  $\varphi_{bm}(d)$ , where  $d$  is the contact diameter]. Situation with an explanation of the inverse connection between the measured barrier height and the ideality factor seems to be more complicated, since it is observed for

contacts of the same type fabricated at the similar conditions. However this situation can be easily designed artificially, if we assume that for the contacts of the same type, there is a certain fluctuating parameter that influences the measured parameters  $n$  and  $\phi_{bm}$ . For example, if the impurity concentration in the semiconductor changes, then the electric field near the contact also changes, which causes in turn the changes in the influence of the image force and barrier transmission coefficient on the IVC. This means that IVC parameters  $n$  and  $\phi_{bm}$  also change as the impurity concentration changes. In other words, the fluctuation of doping level over semiconductor surface causes the fluctuations of the measured parameters of SBCs fabricated on different places of the surface, whereas the relation between these parameters is still determined by Eq. (7) regardless of doping level. Note, that the impurity concentration is the only factor for the considered ideal contact, which can cause the fluctuation of the measured contact parameters. The number of these factors is significantly larger in real contacts. These factors are, for example, the characteristics of the interface states, intermediate layer, and others.

Numerical quantities chosen for the calculation correspond to gallium arsenide SBDs:  $R^* = 8.16 \text{ A/cm}^2\text{deg}$ ,<sup>2</sup>  $\phi_b^0 = 0.8 \text{ V}$  is the barrier height without taking into consideration the image force effect (this value lies approximately in the middle of the region of the real barrier heights<sup>1</sup>),  $N_C = 4.7 \cdot 10^{17} (T/300)^{3/2} \text{ cm}^{-3}$ ,  $m^* = 0.068m_0$  is the effective electron mass ( $m_0$  is a free electron mass),  $\epsilon_{sr} = 12.4$  is the relative permittivity of the semiconductor. The contact diameters were selected in the wide range from submicrons to hundreds of microns. However, it is necessary to take into account that real dependences  $n(d)$  and  $\phi_{bm}(d)$  should be significantly enhanced with the decrease of the contact diameter due to the contribution from the peripheral tunnel effect, which was not considered here.<sup>17</sup> Basic dependences are given for the current value  $I = 10^{-6} \text{ A}$ , at which the SBC parameters are usually measured in practice, and impurity concentration  $4 \times 10^{16} \text{ cm}^{-3}$ , for which the significant enhancement of the tunnel effect begins at temperatures below 100K. The influence of impurity concentration was estimated in the range of  $5 \times 10^{14}$  to  $2.5 \times 10^{18} \text{ cm}^{-3}$ .

Figure 1(a) shows the IVCs calculated according to Eqs. (1)–(3) for two contact diameters (500 and  $5 \mu\text{m}$ ). The plots of the ideality factor versus the current [Fig. 1(b)] indicate directly the nonlinear bias dependence of the effective barrier height, which reveals itself in the availability of the  $n = n(\log I)$ -dependence [see Eqs. (5) and (5A)]. The effect can be particularly significant for contacts with small diameters at low temperature which is due to the application of larger bias voltage to maintain the current constancy during measurements (see also Fig. 2). The average ideality factor in the current range ( $10^{-6}$ – $10^{-4}$ ) A for example given in Fig. 1(b) ( $d = 5 \mu\text{m}$ ,  $T = 77\text{K}$ ) is defined with the accuracy of about  $\pm 0.05$ . For larger contacts at higher temperatures, this uncertainty drops quickly to the level of the usual measurement error.

Note that absolute values of a series resistance  $R_s$  were selected arbitrarily ( $R_s = 1 \Omega\text{m}$  for the contact diameter 500 microns). Only the correspondence of the  $R_s$  values to the

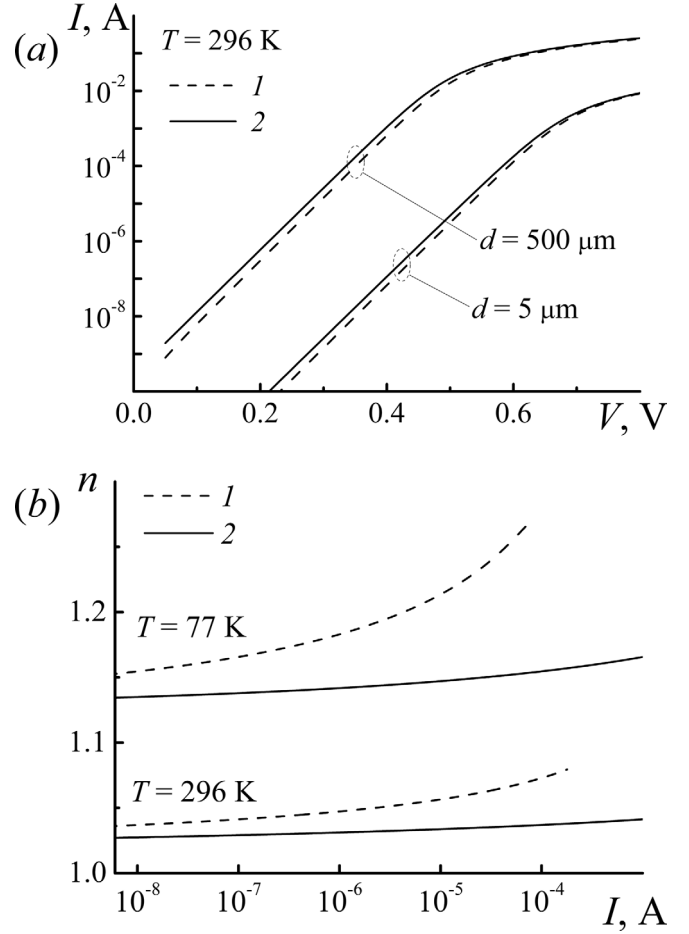


FIG. 1. (a) IVCs of m-n-GaAs SBC with different diameters at 296K considering the influence of image forces only (line 1) and summery effect of image forces and tunneling (line 2); (b) plots of ideality factor versus current for contacts with diameters of  $5 \mu\text{m}$  (line 1) and  $500 \mu\text{m}$  (line 2) at temperatures 296K and 77K ( $\phi_b^0 = 0.8 \text{ V}$ ,  $N_D = 4 \times 10^{16} \text{ cm}^{-3}$ ).

relations between the contact diameters was taken into account.

Figures 2(a) and 2(b) show (for temperatures 296 and 77K) the bias dependences of the ideality factor and measured and effective barrier heights calculated from IVC according to Eqs. (5), (7), (9), and (10) without (curve 1) and with (curve 2) allowance for the tunneling in the contact. Here and afterwards, the barrier height scale is indicated with the symbol  $\phi_b$ . We recall, that in the absence of real tunneling the effective barrier height corresponds to the real barrier height  $\phi_{bi}$  (see Sec. II). Figure 2 shows also the dependences for the quantity  $\phi_{bn} = n\phi_{bm}$  considering the tunnel effect. The  $\phi_{bn} = n\phi_{bm}$  is in fact, the approximate value of the effective barrier height  $\phi_{bl}$ , as can be seen from Eq. (7). This circumstance explains the fact that the  $\phi_{bn} = n\phi_{bm}$  was used by some researchers as the evaluative magnitude of the real barrier height.<sup>8,36</sup>

As can be seen from Fig. 2, in both cases, that is without and with allowance for the tunnel effect, the nonlinear character of the bias dependence of the effective barrier height is revealed. As a consequence, oppositely directed change of parameters  $n$  and  $\phi_{bm}$  with the bias increase is observed. At low temperature [Fig. 2(b)], the changes in parameters  $n$  and



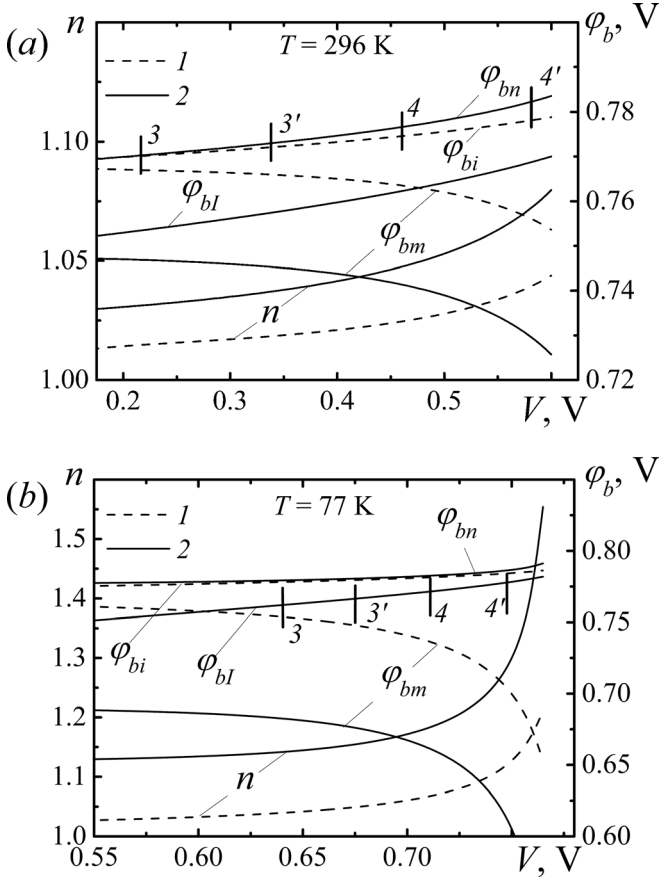


FIG. 2. Plots of ideality factor  $n$ , measured ( $\phi_{bm}$ ), real ( $\phi_{bi}$ ) and effective ( $\phi_{bl}$ ) barrier heights and value  $\phi_{bn} = n\phi_{bm}$  versus bias voltage considering the influence of image forces only (line 1) and summary effect of image forces and tunneling (line 2): (a) –  $T = 296$  K, (b) –  $T = 77$  K; bias voltage ranges 3–3' and 4–4' correspond to the current range ( $10^{-6}$  to  $10^{-4}$ ) A for contacts with diameters of 500 and 5  $\mu\text{m}$ , respectively ( $\phi_b^0 = 0.8$  V,  $N_D = 4 \times 10^{16} \text{ cm}^{-3}$ ).

$\phi_{bm}$  are expressed more strikingly, since in this case, measurements are made at greater bias voltages to maintain the constant current regime, where the dependences  $\phi_{bl}(V)$  and  $\phi_{bi}(V)$  are more steep functions. Bias voltage ranges limited by the line sections 3–3' and 4–4' correspond to the above-mentioned measurement current range ( $10^{-6}$  to  $10^{-4}$ ) A for contact diameters 500 and 5  $\mu\text{m}$ , respectively. Evidently, the influence of the barrier height nonlinearity increases as the contact diameter decreases. Note also the close coincidence of values  $\phi_{bn} = n\phi_{bm}$  and  $\phi_{bi}$  in all the bias voltage ranges both at room and low temperatures. The difference between them does not exceed 5 mV.

Figure 3 demonstrates the behavior of analyzed characteristics in the temperature range. First of all, one can see the oppositely directed change of parameters  $n$  and  $\phi_{bm}$  in the whole range. Such behavior corresponds to the so-called “low temperature anomaly” in real SBCs discussed in introduction. In the absence of tunneling (considering only the image force effect, curve 1), the nonlinearity of the barrier height  $\phi_{bi}(V)$  is the only cause of the “anomaly.” Considering the tunnel effect alone (curve 2), the  $\phi_{bl}(V)$  nonlinearity enhances the “anomalous” behavior of parameters  $n$  and  $\phi_{bm}$ . Such behavior is explained by the tunnel current mech-

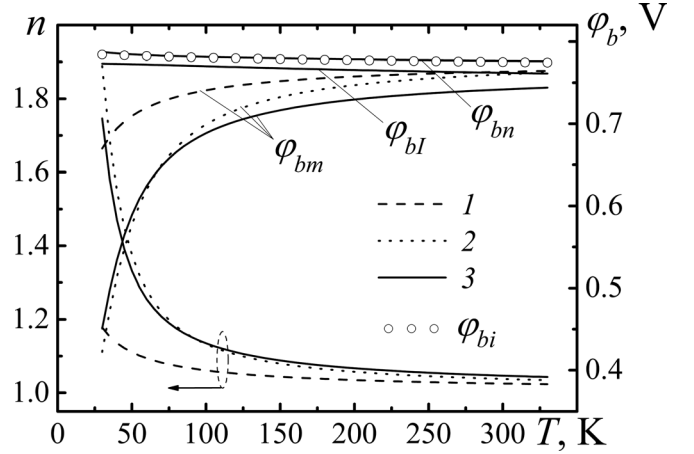


FIG. 3. Temperature dependences of the ideality factor  $n$ , the barrier heights (measured  $\phi_{bm}$ , effective  $\phi_{bl}$ , real  $\phi_{bi}$ ) and value  $\phi_{bn} = n\phi_{bm}$  for contact m-n-GaAs considering the influence of image forces only (line 1), tunnel effect only (line 2) and summary effect (line 3) ( $\phi_b^0 = 0.8$  V,  $N_D = 4 \times 10^{16} \text{ cm}^{-3}$ ,  $I = 10^{-6}$  A,  $d = 500 \mu\text{m}$ ).

anism itself.<sup>31,33</sup> Curve 3 depicts the result of a summary effect of the image force and tunneling on the behavior of parameters. Evidently, at specified doping density ( $N_D = 4 \times 10^{16} \text{ cm}^{-3}$ ), the influence of image force is relatively small and decreases with temperature decreasing.

Special attention is drawn to the fact that the changes of the effective barrier height  $\phi_{bl}$  and the value of  $\phi_{bn} = n\phi_{bm}$  with temperature decrease are similar to that for real barrier height,<sup>1</sup> that is, they do not have the anomalous decrease. Amazing is the circumstance that the value of  $\phi_{bn}$  practically coincides with high accuracy with the real (physical) barrier height  $\phi_{bi}$  in all the temperature range (same as in the bias voltage range, Fig. 2). The numerical verification showed that value of:

$$\phi_{bi}(V) = \phi_b^0 - \Delta\phi_{bi}(V) = \phi_b^0 - a(\phi_b^0 - \phi_s - V)^{1/4} \quad (11)$$

where  $a = (q^3 N_D / 8\pi^2 \epsilon_s^3)^{1/4}$  and  $\Delta\phi_{bi}$  is the barrier height decrease caused by the image force effect, calculated in accordance with the known constant field approximation<sup>1</sup> coincides very closely with the value of  $\phi_{bi} = V_m + \phi_s$  calculated from the potential profile in the barrier (see Sec. II). The coincidence of  $\phi_{bn}$  and  $\phi_{bi}$  allows, referring to expression (6), which is true for any bias (current) and equivalent to the expression:

$$I = AR^*T^2 \exp\left(-\frac{q\phi_{bn}}{nkT}\right) \exp\left(\frac{qV}{nkT}\right), \quad (12)$$

to represent with high accuracy the IVC of the considered contact in the form:

$$I = AR^*T^2 \exp\left(-\frac{q\phi_{bi}}{nkT}\right) \exp\left(\frac{qV}{nkT}\right). \quad (13)$$

Such representation of IVC was discussed earlier in works devoted to ideal<sup>30</sup> and tunnel contacts.<sup>31</sup> It should be said that the cause of such close coincidence of values  $\phi_{bn}$  and  $\phi_{bi}$  is not obvious. Probably, it is related to the similar (or

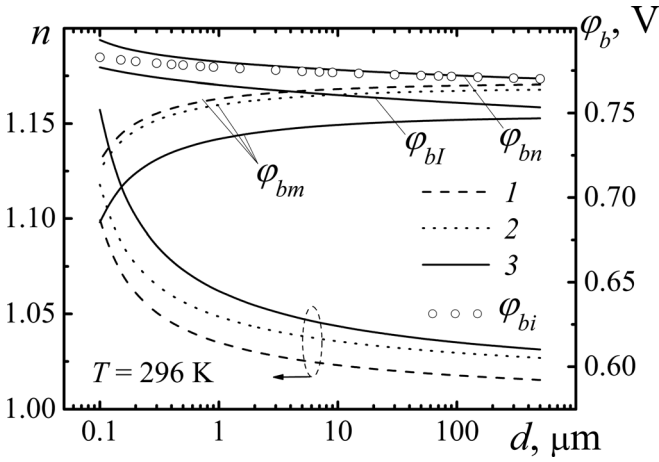


FIG. 4. The ideality factor  $n$ , the barrier heights (measured  $\phi_{bm}$ , effective  $\phi_{bl}$ , real  $\phi_{bi}$ ) and the value  $\phi_{bn} = n\phi_{bm}$  for SBC m-n-GaAs versus contact diameter considering the influence of image forces only (line 1), tunnel effect only (line 2) and summary effect (line 3) ( $\phi_b^0 = 0.8$  V,  $I = 10^{-6}$  A,  $N_D = 4 \times 10^{16}$  cm $^{-3}$ ).

close) character of influence of the image force and tunneling on the barrier height (in case of tunneling – effective barrier height).

As it is known, IVCs of real contacts sometimes are also presented in the form like Eq. (12) (see, for example, Refs. 8, 16, 35, and 36). The reason is that the barrier height  $\phi_{bn}$  determined from this IVC is close to the real one (defined by C-V-method) and does not have temperature anomalies. This circumstance is an important indication to the principal similarity of the “low temperature anomaly” mechanism in the ideal and real contacts, the basis of which, in our opinion, is the nonlinear bias dependence of the effective barrier height.

Figure 4 demonstrates a new effect of the barrier height nonlinearity. It reveals itself in the oppositely directed changes of measured parameters  $n$  and  $\phi_{bm}$ , ideality factor increase and the measured barrier height decrease with the contact diameter decrease. Essentially, we are dealing with the exhibition of the edge effects in the contacts with small diameters. The nature of this effect arises from the displacement of current range, within which parameters  $n$  and  $\phi_{bm}$  are measured, to the range of higher bias voltages, as the contact diameter decreases (see Fig. 2). As a result, the steepness of  $\phi_{bl}(V)$ -function increases at higher voltages, which causes changes of values  $n$  and  $\phi_{bm}$  according to (5), (6), and (10) [see also comments to Fig. 1(b) above]. Evidently, the decrease of temperature and contact diameter have a similar effect on the behavior of measured parameters in such SBCs.

Note one important circumstance. The behavior of measured parameters in the range of submicron contacts was simulated under the same conditions as for large contacts (one-dimensional case). However in fact, because of the added current component caused by the peripheral tunneling, the role of which is greater, the smaller the contact diameter is, the change of values  $n$  and  $\phi_{bm}$  in this range can be expressed much stronger (see, for example, Ref. 17). As for behavior of barrier heights  $\phi_{bl}$ ,  $\phi_{bi}$ , and  $\phi_{bn}$ , it is similar to the observed one in temperature dependences in Fig. 3.

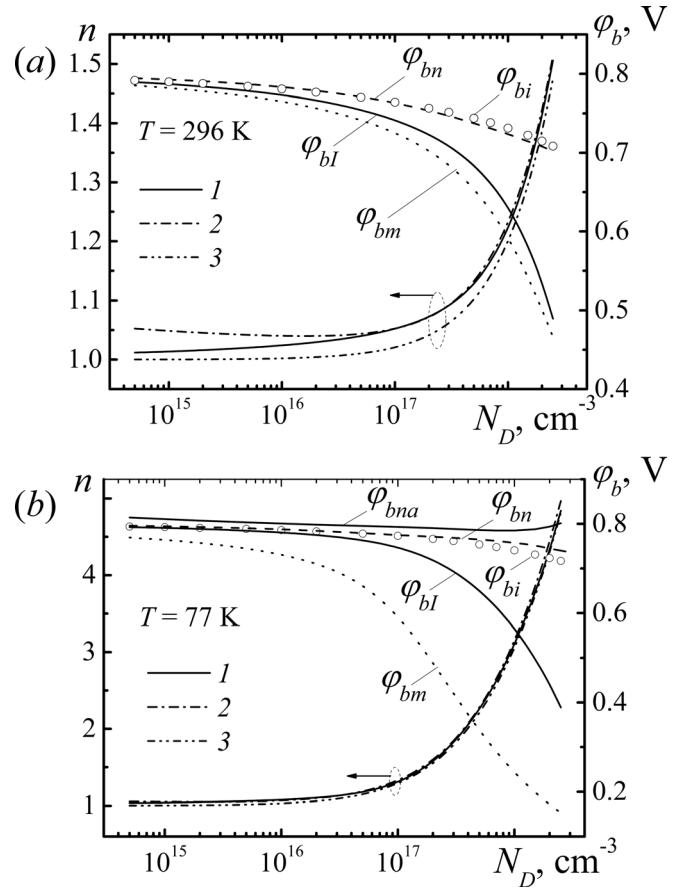


FIG. 5. The ideality factor  $n$ , the barrier heights (measured  $\phi_{bm}$ , effective  $\phi_{bl}$ , real  $\phi_{bi}$ ), values  $\phi_{bn} = n\phi_{bm}$  and  $\phi_{bna} = n_a\phi_{ba}$  for SBC m-n-GaAs vs doping level, considering the summary influence of the image force and the tunneling effects: (a) –  $T = 296$  K; (b) –  $T = 77$  K; (line 1) values  $n$  calculated from Eq. (5); (line 2) values  $n$  according to the first approximation in (15); (line 3) according to the second approximation in (15) ( $I = 10^{-6}$  A,  $d = 50$  μm).

Value  $\phi_{bn}$  is still very close to the real (physical) barrier height  $\phi_{bi}$ , which means that the expression (13) for IVC remains to be valid in this case also.

Thus, one can state that at least one of the reasons of edge effects in SBCs can be not the influence of the periphery, but the fundamental property of the contact: nonlinear bias dependence of its barrier height. Though in real contacts, this nonlinear property can be caused by technological and constructive reasons and can be expressed more brightly.

Figure 5 shows the behavior of the measured contact parameters versus semiconductor doping level in the impurity concentration range  $5 \times 10^{14}$  to  $2.5 \times 10^{18}$  cm $^{-3}$  at room temperature and temperature of liquid nitrogen: Fig. 5(a) and Fig. 5(b), respectively. It was taken into account in the calculation that with impurity concentration close to  $10^{18}$  cm $^{-3}$  the semiconductor already becomes degenerate one at room temperature.<sup>1</sup> Because of this the Fermi-level position in n-GaAs was determined by a numerical solution of the charge neutrality equation.<sup>28</sup> The Fermi-Dirac carrier distribution was also used at calculating current through the contact according to Eq. (1). Note, that dependences on Fig. 5 are specified for the contact diameter 50 μm, since the diameter increase limits

from above the range of permissible impurity concentrations at room temperature. The matter is that the current increase with the increase of the impurity concentration (as the result of tunneling) makes it impossible to determine (calculate) measured parameters in the selected range of currents ( $10^{-6}$  to  $10^{-4}$ ) A for too high doping levels at high (296K) temperatures. The upper boundary for the impurity concentration corresponds to  $N_D \cong 10^{18} \text{ cm}^{-3}$  at  $d = 500 \text{ }\mu\text{m}$ .

Special attention must be given to the fact that the barrier height  $\phi_{bn}$  with high accuracy corresponds to the real (physical) barrier height  $\phi_{bi}$  just as in dependences on the temperature and contact diameter (Fig. 3 and Fig. 4). The maximum difference between them does not exceed 10 mV in all the concentration range at the room temperature. At temperature of the liquid nitrogen, Fig. 5(b), the maximum difference between  $\phi_{bn}$  and  $\phi_{bi}$  (note, with the opposite sign) is also negligible (lower 6 mV) up to impurity concentration  $2 \times 10^{17} \text{ cm}^{-3}$  and increases smoothly till  $\sim 23 \text{ mV}$  at  $N_D = 2 \times 10^{18} \text{ cm}^{-3}$ . The diameter increase, at least up to 500 microns, practically does not change this situation, if one disregards some decrease of the considered range of impurity concentrations with the diameter increase, which was mentioned above.

Note also, that the substitution of the Maxwell-Boltzmann carrier distribution for the Fermi-Dirac distribution in Eq. (1) in order to take into account the degeneration in semiconductor (see above) gives the effect, which is greater, the higher the impurity concentration is and lower the temperature is. At 296 K, this effect expressed as the difference in  $\phi_{bn}$  values for both cases is insignificant. It does not exceed 3 mV for the highest impurity concentration  $2.5 \times 10^{18} \text{ cm}^{-3}$ . At 77 K, the difference in  $\phi_{bn}$  becomes noticeable ( $\sim 3 \text{ mV}$ ) at  $N_D = 2 \times 10^{17} \text{ cm}^{-3}$  and increases smoothly with concentration increase:  $\sim 8 \text{ mV}$  and  $\sim 17 \text{ mV}$  at  $N_D = 10^{18} \text{ cm}^{-3}$  and  $2 \times 10^{18} \text{ cm}^{-3}$ , respectively.

All mentioned above, considering the results displayed on Figs. 3 and 4, implies that the IVC of the discussed SBC (with the predominant influence of image force and tunneling) can be presented in the very simple analytical form (13) in the wide range of temperatures, impurity concentrations and contact diameters. It is obvious that the expression (13) gives reasons for equally simple and accurate method of defining the barrier height in real SBCs with predominantly tunnel current in accordance with Eq. (11) and Fig. 5:  $\phi_b^0 = \phi_{bi} + \Delta\phi_{bi} \cong \phi_{bn} + \Delta\phi_{bi}$ , where  $\phi_{bn} \equiv n\phi_{bm}$  is determined by directly measured values  $n$  and  $\phi_{bm}$  at specified current (or narrow current range). For carrying out measurements, the SBCs with impurity concentration more than  $10^{17} \text{ cm}^{-3}$  should be used to enhance the tunnel current. In this case the role of contact imperfection, which can effect the ideality factor, can be reduced significantly.

It is important that the  $\Delta\phi_{bi}(N_D)$  plot, displayed in the Fig. 6, not only depends slightly on the current in current range ( $10^{-6}$  to  $10^{-4}$ ) A (not shown in the figure) but does not depend on the barrier height at all. This is due to the fact, that the barrier height increase (or decrease) resulting in a decrease (or an increase) of the current through the contact, is compensated by the bias voltage chosen [see Eq. (11)] to meet the condition of the current constancy at the measure-

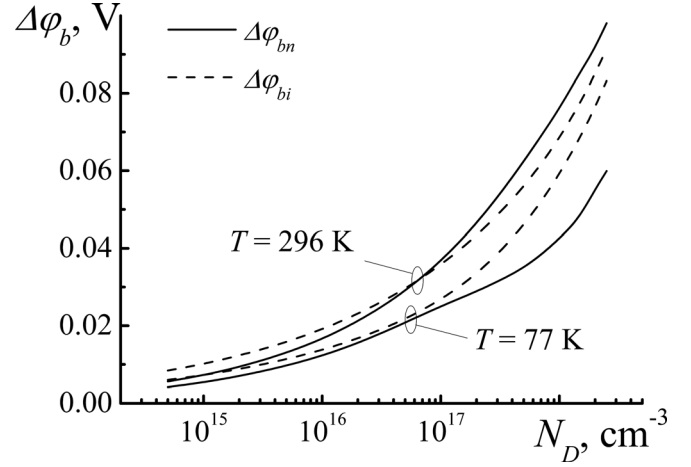


FIG. 6. The  $\Delta\phi_{bi}(N_D)$  and  $\Delta\phi_{bn}(N_D)$  dependences, defined according to (11) and (14), respectively, at 296K and 77K ( $\phi_b^0 = 0.8$ ,  $I = 10^{-6} \text{ A}$ ,  $d = 50 \text{ }\mu\text{m}$ ).

ments for contacts with different barrier heights. Thus, the calculated  $\Delta\phi_{bi}(N_D)$  dependence along with the value of  $\phi_{bn}$  determined from the IVC completely define the barrier height  $\phi_b^0 \cong \phi_{bn} + \Delta\phi_{bi}$  at specified impurity concentration, temperature and permittivity. As it was shown, the current decrease below  $10^{-6} \text{ A}$  practically does not change the magnitude  $\Delta\phi_{bi}(N_D)$ , so the defined barrier height  $\phi_b^0$  can be referred reasonably to  $V = 0$ .

As it turned out, the  $\Delta\phi_{bn}(N_D)$  dependence exhibits practically the same properties as the  $\Delta\phi_{bi}(N_D)$ , Fig. 6. The magnitude  $\Delta\phi_{bn}(I)$  at specified current was calculated from relationship

$$\Delta\phi_{bn}(I) = \phi_b^0 - \phi_{bn}(I) \quad (14)$$

for  $\phi_b^0 = 0.8$ . Its independence from the barrier height  $\phi_b^0$  means that Eq. (12), coupled with the  $\Delta\phi_{bn}(N_D)$  dependence calculated according Eq. (14) for any barrier height at specified impurity concentration, temperature, and permittivity, makes it possible to propose still more precise method for determining the barrier height  $\phi_b^0$  using measured parameters  $n$  and  $\phi_{bn} = n\phi_{bm}$  and calculated magnitudes  $\Delta\phi_{bn}(N_D)$ , Fig. 6. The precision of so defined barrier height depends only on experimental accuracy of  $n$  and  $\phi_{bm}$  measurements and the deviation from the current constancy condition, influence of which [in limits ( $10^{-6}$  to  $10^{-4}$ ) A] is insignificant, as numerical evaluations show.

Naturally, these methods can be used at any temperature with the availability of the calculated  $\Delta\phi_{bi}(N_D, T)$  or  $\Delta\phi_{bn}(N_D, T)$  dependencies, which are presented for two temperatures 296 and 77K in Fig. 6. One can see, that the change of the  $\Delta\phi_{bi}(N_D, T)$  in all temperature range is only about 10 mV. Variations of  $\Delta\phi_{bi}$  and  $\Delta\phi_{bn}$  in temperature interval  $(296 \pm 5) \text{ K}$  does not exceed 1 mV.

Figures 5(a) and 5(b) also display plots of known approximations for the ideality factor of the tunnel contact for the comparison to accurate dependences  $n(N_D)$ , calculated from the IVC according to Eq. (5). These approximations are:<sup>33,34</sup>

$$n = \frac{q}{kT} \left[ \frac{th(qE_{00}/kT)}{E_{00}} - \frac{1}{2(\varphi_b^0 - \varphi_s - V)} \right]^{-1} \text{ and} \quad (15)$$

$$n = \frac{E_{00}}{kT} cth\left(\frac{qE_{00}}{kT}\right),$$

where

$$E_{00} = \frac{qh}{4\pi} \left( \frac{N_D}{m^* \varepsilon_s} \right)^{1/2}. \quad (16)$$

As one can see, the first expression in (15), which considers the  $n$  dependence on bias voltage, is a good approximation for the ideality factor at the room temperature for impurity concentrations  $> 5 \times 10^{16} \text{ cm}^{-3}$ . At low temperatures both expressions in Eq. (15) show more than satisfactory agreement with the values  $n$  calculated from the IVC.

It is also interesting to compare our IVC approximation (13) with the known analytical approximation for the IVC of the tunnel contact received in Ref. 33, when the integrand in Eq. (1) was approximated by the Gaussian distribution, disregarding the image force effect (see also Refs. 37 and 38). According to Ref. 33 the approximated expression for the IVC can be presented as follows:

$$I = AR^*T^2 \exp\left(-\frac{q\varphi_s}{kT}\right) \frac{[\pi E_{00} E_b th(E_{00}/kT)]^{1/2}}{kTch(E_{00}/kT)} \times \exp\left[-\frac{E_b}{E_{00}} th\left(\frac{E_{00}}{kT}\right)\right], \quad (17)$$

where  $E_b = q(\varphi_b^0 - \varphi_s - V)$ . Presenting this characteristic in the form similar to (6) and (12),

$$I = AR^*T^2 \exp\left[-\frac{q\varphi_{bna}(V)}{kT}\right] \exp\left(\frac{qV}{n_a kT}\right) = AR^*T^2 \exp\left[-\frac{q\varphi_{bna}(V)}{n_a kT}\right] \exp\left(\frac{qV}{n_a kT}\right), \quad (18)$$

where  $\varphi_{bna} = n_a \varphi_{bma}$ , and making it equal to the IVC (17) at the specified current (similar to the procedure that was accepted above at the definition of  $n$  and  $\varphi_{bm}$ ) it is not difficult to define numerically at this current the values of the measured barrier height  $\varphi_{bma}$ , the barrier height  $\varphi_{bna}$  and the ideality factor  $n_a$ , which practically corresponds to the first expression in (15) according to Ref. 33.

The results of comparing  $\varphi_{bna}$  with calculated values  $\varphi_{bn} = n\varphi_{bm}$  from the integral IVC (1) show that at room temperature the analytical approximation (17) should be regarded as unsatisfactory: the difference  $\varphi_{bna} - \varphi_{bn}$  in all the range of impurity concentrations lies within  $\sim(40 - 100)$  mV. At 77K, the approximation (17) is much better, Fig. 5(b), but in this case it is also essentially worse than the approximation (13), as it follows from the comparison of curves, corresponding to  $\varphi_{bn}$ ,  $\varphi_{bi}$ , and  $\varphi_{bna}$ . It is obvious that the increase in the accuracy of the approximation (17) with the decrease of temperature is due to the decrease of the image force effect role (it was not considered in Ref. 33) in conditions, when the role of tunneling increases.

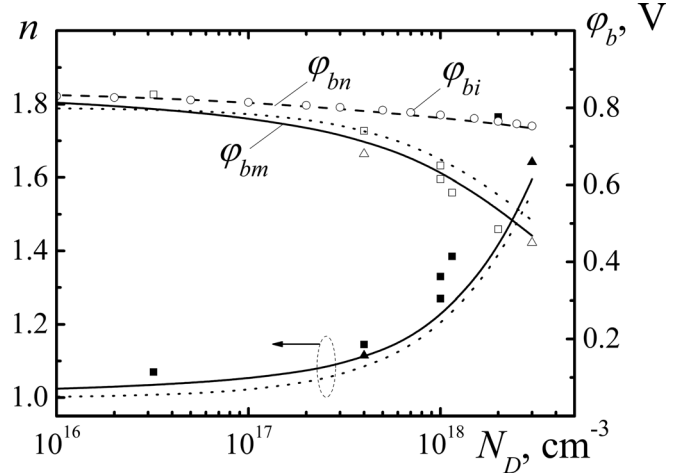


FIG. 7. Measured and calculated barrier heights and ideality factors of Pt-Ti-GaAs contacts versus doping concentration: square and delta filled dots are measured  $n$  values for epitaxial and bulk material, respectively (see Ref. 39); square and delta open dots are measured  $\varphi_{b0}$  values for epitaxial and bulk material, respectively (see Ref. 39); dotted lines are the  $n(N_D)$  and the  $\varphi_{b0}(N_D)$  plots from Ref. 39, calculated in accordance with the second Eq. in (15) and Eq. (8), respectively; solid lines are the  $n(N_D)$  and the  $\varphi_{bm}(N_D)$  plots from our calculation in accordance with Eq. (5) and Eq. (10), respectively; dashed lines are  $\varphi_{bn} = n\varphi_{bm}$ ; open circles are  $\varphi_{bi} = \varphi_b^0 - \Delta\varphi_{bi}$ ; [ $I = 10^{-6}$  A,  $S = 5.625 \cdot 10^{-3} \text{ cm}^2$  (Ref. 39)].

The experimental verification of the validity of the obtained  $I$ - $V$ -characteristic in the form (12) or (13) is a rather tedious task. However, there is a possibility to make use of the known experimental results for the Pt-Ti-n-GaAs contacts for this purpose.<sup>39</sup> They are presented in Fig. 7. Here the filled points correspond to measured ideality factors according to Eq. (5), and the open points correspond to measured barrier heights according to Eq. (10) versus a doping level of the semiconductor. The delta points pertain to contacts with bulk material, and the square points pertain to epitaxial material. The calculated dependences  $n(N_D)$  in accordance with the second expression in (15), and  $\varphi_{b0}(N_D)$  obtained from Eq. (8), with  $\varphi_{bf}$  taken equal to the optimized value of 0.8 V and  $n$  taken from calculated  $n(N_D)$  dependence, are shown by dotted lines. According to Ref. 39 the  $\varphi_{b0}$  value from Eq. (8) equals to measured barrier height  $\varphi_{bm}$  [according to Eq. (10)].

The continuous lines in Fig. 7 depict similar dependencies obtained by us from calculated  $I$ - $V$ -characteristics for different doping concentrations. The barrier height  $\varphi_{b0} \equiv \varphi_b^0$  [see Eqs. (8) and (11)] was taken equal to 0.85 V, since there is no reliable information about  $\varphi_b^0$  in Ref. 39. It corresponds to the data for single-type contacts Au-Ni-Ti-n-GaAs,<sup>40</sup> obtained by  $I$ - $V$ - and  $C$ - $V$ -methods for  $N_D \approx 10^{16} \text{ cm}^{-3}$  at  $n = 1.02 - 1.03$ . In our case the  $n(N_D)$  dependence was calculated from the tangent (6) according to Eq. (5) at  $I = 10^{-6}$  A, and the  $\varphi_{bm}(N_D)$  dependence was calculated from the same tangent according to Eq. (10) for different doping concentrations. Both of these values enter directly in IVC (12) and correspond to measured ones from experimental IVCs. The comparison of calculated and measured results shows that proposed IVC (13) for the tunnel contact, in which  $\varphi_{bi} \simeq \varphi_{bn}$ , really agrees closely with experimental results for a wide range of doping concentrations in semiconductor.



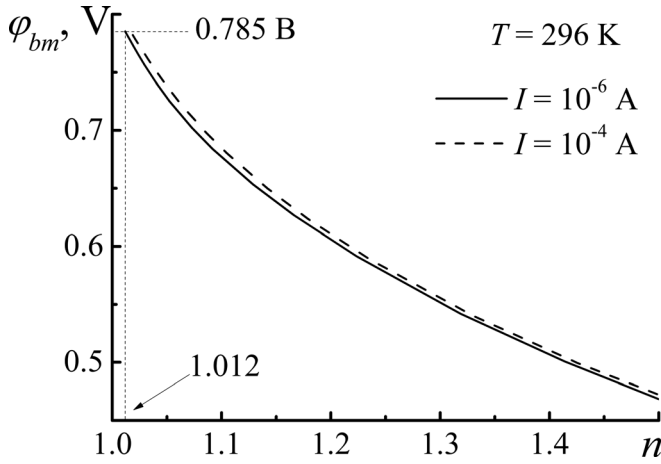


FIG. 8. The inverse connection between the ideality factor  $n$  and the measured barrier height  $\varphi_{bm}$  (defined from Eq. (7) for contacts with different impurity concentrations) reflecting the influence of the doping level fluctuations in single-type contacts on the values  $n$  and  $\varphi_{bm}$  ( $\varphi_b^0 = 0.8$  V,  $d = 50$   $\mu\text{m}$ ).

The equality  $\varphi_{bi} \simeq \varphi_{bn}$  is confirmed directly by coincidence of the calculated  $\varphi_{bn}(N_D)$  and  $\varphi_{bi}(N_D)$  dependences shown in Fig. 7, where  $\varphi_{bn} = n\varphi_{bm}$  and  $\varphi_{bi} = \varphi_b^0 - \Delta\varphi_{bi}$  with  $\varphi_b^0 = 0.85$  B.

Note, that, strictly speaking, it is not correct to use the barrier height  $\varphi_{b0}$  from Eq. (8) (dotted line) for comparison with measured barrier heights from experimental IVCs, as it was done in Ref. 39. The notion of the flat-band barrier height, Eq. (8), was introduced for contacts with the intermediate layer,<sup>1</sup> and it is not applicable to tunnel contacts. In the latter case the barrier heights at zero bias and at flat-band conditions are equal to each other (without taking into account the image force effect). The matter is that the tunnel contact is intimate contact, whose ideality factor is determined by tunnel effect and not by intermediate layer.<sup>1</sup>

We suppose, that the observed agreement between the  $\varphi_{b0}(N_D)$  dependence (dashed line) and measured barrier heights (open dots) in Ref. 39, Fig. 7, is connected with similarity of the IVCs [in the form (12)] for all contacts, which behavior is significantly affected by the nonlinear bias dependence of actual or effective barrier height. Among these are tunnel contacts,<sup>31</sup> contacts with intermediate layer and interface states,<sup>27</sup> intimate contacts with subsurface states,<sup>28</sup> inhomogeneous contacts<sup>29</sup> and possibly others.

Finally, Fig. 8 demonstrates the inverse connection between the values  $\varphi_{bm}$  and  $n$  (described in the beginning of this section) which is constructed on the basis of the results presented in Fig. 5(a), where each pair of “connected” values  $\varphi_{bm}$  and  $n$  corresponds to certain magnitude of the impurity concentration. Practically, we speak about the comparison of contacts with different impurity concentrations, and this comparison gives the comprehensive idea of the relation between the measured barrier height and ideality factor in the single-type contacts with the availability of the impurity concentration fluctuations in semiconductor. The relation between  $\varphi_{bm}$  and  $n$  shown on the figure, is quite predictable. As one can see, with the decrease of the impurity concentration to the level of  $5 \times 10^{14} \text{ cm}^{-3}$ , the ideality factor tends to the value that is due to the influence of image force only

( $n_i \simeq 1.012$ ), and the measured barrier height (0.785 V) tends to the real barrier height  $\varphi_{bi} = 0.789$  V. The selection of the contact diameter insignificantly influences the final result. Its increase up to 500  $\mu\text{m}$  results in changing in the ideality factor  $n_i$  for  $\sim 0.003$  and barrier heights for  $\sim 1$  mV.

As it is known, the method of determining the real barrier height in SBCs proposed in works<sup>6,41</sup> is based on the relation between  $n$  and  $\varphi_{bm}$ , specifically, on the transformation of the measured barrier height to the real one  $\varphi_{bi}$  at the transformation of  $n$  to the value  $n_i$  corresponding to the influence of image force only. It was assumed that this relation is caused by barrier height fluctuations in the form of “saddle points.” As one can see, the connection between  $n$  and  $\varphi_{bm}$  can also appear as the result of doping level fluctuations in the ideal contact. For real SBCs, quite probable reasons of similar connection between  $n$  and  $\varphi_{bm}$  are the fluctuations of parameters of the intermediate layer and interface states and some others.

Figure 8 gives also one more possibility to make sure that the influence of the specified current (in the range  $10^{-6}$  to  $10^{-4}$  A) on the dispersion of measured values of the barrier height, and the ideality factor is insignificant.

#### IV. CONCLUSION

In this work the reasons of the “anomalous” behavior of SBC IVCs in the range of low temperatures (the “low temperature anomaly”), at small contact diameters (edge effects) and reasons of inverse connection between the measured barrier height and ideality factor of single type contacts are considered on the example of the ideal contact m-n-GaAs, where basic influence factors on IVC are image force and tunneling. The numerical analysis shows that all these “anomalies” phenomena can be described and explained on the basis of the notion about the nonlinear bias dependence of the barrier height (generally, effective one) providing that the SBC parameters are determined at specified current value in the temperature or contact diameter ranges.

One more principal result of the analysis is the evidence that the IVC of this contact type in a wide range of temperatures, impurity concentrations and contact diameters can be described with the simple Eq. (13), which contains the real (physical) barrier height (considering the image force effect) and directly measured ideality factor. This conclusion was confirmed by comparison with known experimental results. This means also that the new and simple method to determine the barrier height in tunnel contacts can be proposed based on the Eq. (13). The accuracy of the method can be improved in certain conditions with using the Eq. (14) ( $\varphi_b^0 = \varphi_{bn} + \Delta\varphi_{bn}$ ), where the quantity  $\varphi_{bn} = n\varphi_{bm}$  is determined directly from the IVC (12) and  $\Delta\varphi_{bn}$  is the calculated value depending on the temperature and impurity concentration.

With having regard to the presented and received earlier results (see Refs. 27–29), one can state that the model of SBC considering the nonlinear bias dependence of the barrier height, can be the basis for the adequate description and explanation of “anomalous” properties of both ideal (in the sense explained above) and real contacts. It seems to be evident that the specific mechanisms that cause the nonlinear

dependence of barrier height can be quite different in different contacts. A special publication will be devoted to the investigation of exhibition of nonlinear bias dependence of the barrier height in real contact properties.

- <sup>1</sup>E. H. Rhoderick and R. H. Williams, *Metal-Semiconductor Contacts*, 2nd ed. (Clarendon Press, Oxford, 1988).
- <sup>2</sup>E. L. Wall, *Solid-State Electron.* **19**, 389 (1976).
- <sup>3</sup>V. G. Bozhkov and O. Y. Malakhovsky, *Elektron. Tekh. Ser. 2*, **5**, 9 (1987).
- <sup>4</sup>M. Wittmer, *Phys. Rev. B* **42**, 5249 (1990).
- <sup>5</sup>A. Martinez, D. Esteve, J. M. Peyriquer, J. M. Lagorse and D. Dameme, in *Proceedings Manchester Conference Metals-Semiconductor Contacts*, Institute of Physics, London, Conference Series N22 (Institute of Physics, London, 1974), p. 67.
- <sup>6</sup>T. U. Kampen, and W. Monch, *Surf. Sci.* **331-333**, 490 (1995).
- <sup>7</sup>F. A. Padovani and G. G. Sumner, *J. Appl. Phys.* **36**, 3744 (1965).
- <sup>8</sup>R. Hackam, P. Harrop, *IEEE Trans.* **ED-19**, 1231 (1972).
- <sup>9</sup>V. G. Bozhkov, K. I. Kurkan, in *Poluprovodnikovye Pribori s Barrierom Schottky*. (Naukova Dumka, Kiev, 1979) p. 43.
- <sup>10</sup>J. H. Werner and H. H. Guttler, *J. Appl. Phys.* **69**, 1522 (1991).
- <sup>11</sup>M. K. Hudait, P. Venkatesvarlu, S. B. Krupanidhis, *Solid-St. Electron.* **45**, 133 (2001).
- <sup>12</sup>H. Korkut, N. Yildirim, A. Turut, *Microelectron. Eng.* **86**, 111 (2009).
- <sup>13</sup>M. O. Aboelfotoh and K. N. Tu, *Phys. Rev. B* **34**, 2311 (1986).
- <sup>14</sup>M. O. Aboelfotoh, *J. Appl. Phys.* **66**, 262 (1989).
- <sup>15</sup>M. Wittmer, *Phys. Rev. B* **43**, 4385 (1991).
- <sup>16</sup>V. G. Bozhkov, G. F. Kovtunencko, G. M. Surotkina, and L. S. Selina, *Elektron. Tekh. Ser. 2*, **4**, 14 (1978).
- <sup>17</sup>V. G. Bozhkov and A. A. Kaschkan, *Elektron. Tekh. Ser. 2*, **7**, 12 (1981).
- <sup>18</sup>G. S. Visweswaran and R. Sharan *Proc. IEEE* **67**, 436 (1979).
- <sup>19</sup>V. G. Bozhkov, O. Yu. Malakhovsky, *Izv. Vuzov. Fiz.* **26**, 94 (1983).
- <sup>20</sup>V. G. Bozhkov, *Izv. Vuzov. Fiz.* **30**, 29 (1987).
- <sup>21</sup>V. G. Bozhkov and O. Y. Malakhovsky, *Izv. Vuzov. Fiz.* **26**, 101 (1983).
- <sup>22</sup>V. G. Bozhkov, O. Y. Malakhovsky, and A. M. Misik, *Izv. Vuzov. Fiz.* **26**, 97 (1983).
- <sup>23</sup>J. P. Sullivan, R. T. Tung, M. R. Pinto, and W. R. Graham, *J. Appl. Phys.* **70**, 7403 (1991).
- <sup>24</sup>R. T. Tung, *Phys. Rev. B* **45**, 13509 (1992).
- <sup>25</sup>V. G. Bozhkov, *Radiophys. Quant. Electron.* **45**, 381 (2002).
- <sup>26</sup>V. G. Bozhkov and D. J. Kuzyakov, *J. Appl. Phys.* **92**, 4502 (2002).
- <sup>27</sup>V. G. Bozhkov and S. E. Zaitzev, *Radiophys. Quant. Electron.* **47**, 688 (2004).
- <sup>28</sup>V. G. Bozhkov and S. E. Zaitzev, *Russ. Phys. J.* **48**, 1085 (2005).
- <sup>29</sup>V. G. Bozhkov and S. E. Zaitzev, *J. Commun. Technol. Electron.* **52**, 97 (2007).
- <sup>30</sup>V. G. Bozhkov and S. E. Zaitzev, *Russ. Phys. J.* **48**, 312 (2005).
- <sup>31</sup>V. G. Bozhkov and S. E. Zaitzev, *Russ. Phys. J.* **49**, 251 (2006).
- <sup>32</sup>Z. J. Horvath, in *Physics of Semiconductor Devices*, edited by V. Kumar and S. K. Agarwal, (Narosa Publishing House, New Delhi, India, 1998) p. 1085.
- <sup>33</sup>C. R. Crowell and V. L. Rideout, *Solid-State Electron.* **12**, 89 (1969).
- <sup>34</sup>V. L. Rideout and C. R. Crowell, *Solid-State Electron.* **13**, 993 (1970).
- <sup>35</sup>L. F. Wagner, R. W. Joung, and A. Sugerman, *IEEE Electron Dev. Lett.* **EDL-4**, 320 (1983).
- <sup>36</sup>Y. A. Goldberg, E. A. Posse, B. V. Tsarenkov, *Fiz. Tekh. Poluprovodnikov* **5**, 468 (1971).
- <sup>37</sup>F. A. Padovani, R. Stratton, *Solid-State Electron.* **9**, 695 (1966).
- <sup>38</sup>V. I. Strikha, *Teoreticheskie Osnovy Raboty Kontakta Metall-Poluprovodnik* (Naukova dumka, Kiev, 1974).
- <sup>39</sup>R. F. Broom, H. P. Meier, and W. Walter, *J. Appl. Phys.* **60**, 1832 (1986).
- <sup>40</sup>V. G. Bozhkov, G. F. Kovtunencko, G. M. Surotkina, and L. S. Selina, *Electron. Tech. Ser. 2*, **4**, 14 (1978).
- <sup>41</sup>R. F. Schmitsdorf, T. U. Kampen, and W. Monch, *J. Vac. Sci. Technol. B* **15**, 1221 (1997).